ELSEVIER

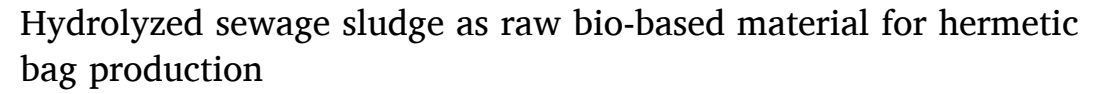
Contents lists available at ScienceDirect

Waste Management

journal homepage: www.elsevier.com/locate/wasman

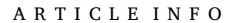


Research Paper



Luis Romero^a, Shihan Weng^a, Paula Oulego^a, Sergio Collado^a, Ismael Marcet^a, Mario Díaz^{a,*}

a Department of Chemical and Environmental Engineering, University of Oviedo, c/Julián Clavería s/n, E-33071 Oviedo, Spain



Keywords:
Bio-based material
Biopolymers
Eco-friendly packaging
Sewage sludge
Thermal hydrolysis

ABSTRACT

This study aimed to assess the potential of sewage sludge, a significant residue of wastewater treatment plants (WWTPs), as a sustainable resource for producing a bio-based material for hermetic bags (BMHB), in order to reduce the dependency on petroleum-derived plastics. The approach involved the application of thermal hydrolysis to solubilize sewage sludge, and it systematically examined critical process parameters, including temperature (120-150 °C), residence time (1-4 h), and medium pH (6.6-10). Results revealed that alkaline thermal hydrolysis significantly enhanced biomolecule solubilization, particularly proteins (289 \pm 1 mg/gVSS₀), followed by humic-like substances (144 \pm 6 mg/gVSS $_{o}$) and carbohydrates (49 \pm 2 mg/gVSS $_{o}$). This condition also increased the presence of large-and medium-sized compounds, thereby enhancing BMHB mechanical resistance, with puncture resistance values reaching 63.7 ± 0.2 N/mm. Effective retention of UV light within the 280-400 nm range was also observed. All BMHB samples exhibited similar properties, including water vapor permeability (WVP) (\sim 3.9 g * mm/m 2 * h * kPa), hydrophilicity (contact angles varied from 35.4° \pm 0.3 to 64° \pm 5), solubility (\sim 95%), and thermal stability (\sim 74% degradation at 700 $^{\circ}$ C). Notably, BMHB proved to be an eco-friendly packaging for acetamiprid, an agricultural pesticide, preventing direct human exposure to harmful substances. Testing indicated rapid pesticide release within 5 min of BMHB immersion in water, with only 5% of BMHB residues remaining after 20 min. Additionally, the application of this material in soil was considered safe, as it met regulatory limits for heavy metal content and exhibited an absence of microorganisms.

1. Introduction

Currently, the use of petroleum-based plastics has significantly raised due to population growth, resulting in a substantial environmental impact (Calva-Estrada et al., 2019). Indeed, the World Economic Forum predicts that by 2050, the quantity of plastic in the ocean could surpass the number of fish, if the current trend continues (World Economic Forum, 2016). In light of this, the search for biodegradable polymers derived from renewable waste materials, instead of those derived from petroleum, is gaining interest as a promising and environmentally friendly option (Shanmathy et al., 2021). To this end, the production of valuable biomaterials from various residual materials, such as leather waste (Chen et al., 2022), Spirulina sp. waste (Zhang et al., 2020), and blood plasma from slaughterhouses (Alvarez et al., 2021), has been analyzed. It is important to note that the significant biopolymer content of these wastes is essential for enabling their transformation into high-value added products. Therefore, it is crucial to evaluate alternative high-content biopolymer wastes and explore pathways to advance sustainable development goals (Adhikary et al.,

In this context, sewage sludge, as the primary residue from wastewater treatment plants (WWTPs), presents a significant concern due to its increasing production. Thus, in the European Union (EU), approximately 13,000 thousand tons (dry matter) of sewage sludge were generated in 2020 (Romero et al., 2023). Various methods are employed for the final disposal of sewage sludge, including land reclamation, incineration, phosphorus recovery and agricultural use; the latter being the most commonly employed approach (EurEau, 2021). Nevertheless, the presence of harmful substances, heavy metals, and pathogens in sewage sludge makes necessary an appropriate processing to render it suitable for such applications (Guleria et al., 2022; Kacprzak et al., 2017). Currently, methane generation is also receiving attention as a means to valorize sewage sludge due to its high organic content (Elalami et al., 2019; Fang et al., 2019; Wang et al., 2018). Nevertheless, this process involves prolonged processing periods and requires strictly controlled conditions (Bien et al., 2004; Gao et al., 2020; Urrea et al.,

E-mail address: mariodiaz@uniovi.es (M. Díaz).

^{*} Corresponding author.

2015). Additionally, pretreatment methods are often needed to enhance methane production, such as ultrasonic treatment, mechanical forces, microwave irradiation, ozonation, Fenton peroxidation, and thermal hydrolysis (Abelleira et al., 2012; Aragon-Briceño et al., 2023). Therefore, it is necessary to evaluate alternatives routes for producing highvalue added products from sewage sludge. In this sense, hydrothermal treatments have been widely studied for their ability to solubilize floc structures within a wide range of temperatures and pressures, releasing a variety of biomolecules of interest, including proteins, carbohydrates and humic acids, through cell lysis and extracellular polymeric substances (García et al., 2017; Hui et al., 2022; Song et al., 2019; Urrea et al., 2018). However, to the best of our knowledge, none of these studies have focused on the use of hydrothermally treated sewage sludge as a biologically derived raw material. This knowledge gap is particularly significant due to the high concentration of biopolymers present in the solubilized solution, thus presenting a promising opportunity for the production of high value-added biomaterials, thanks to the abundance of readily biodegradable compounds (Pola et al., 2022; Thomas et al.,

Based on the abovementioned considerations, the aim of this study was to assess for the first time the use of sewage sludge as a raw bio-based material for the production of hermetic bags (BMHB). To that end, the influence of different operating conditions (temperature, residence time and pH) on the physicochemical properties and particle size distribution of the sewage sludge, solubilized by thermal hydrolysis, was examined. The BMHB samples were completely characterized in terms of mechanical properties, transparency, color, permeability, solubility, wettability, thermal stability, and morphology. Additionally, the concentration of heavy metals and the presence of microorganisms were determined to ensure the safety of this bio-based material. Furthermore, the suitability of the BMHB as a pesticide container for agricultural applications was also evaluated.

2. Material and methods

2.1. Raw bio-based material

Sewage sludge was collected from a secondary sludge thickener at a municipal WWTP located in Asturias (Spain) and stored at 4 °C for a maximum of 10 days before utilization. The main characteristics of this raw material were: total chemical oxygen demand (TCOD): 37169 \pm 43 mg O $_2$ /L, SCOD: 490 \pm 20 mg O $_2$ /L, total suspended solids (TSS): 33.6 \pm 0.1 g/L, volatile suspended solids (VSS): 27.2 \pm 0.1 g/L, and pH: 6.8 \pm 0.2. More details related to the biomolecules and color can be found in the Supplementary material (Table S1).

2.2. Experimental setup

A PARR 4520 series reactor of 1 L capacity, equipped with a single-propeller stirrer and a 2 L steel tank gas humidifier filled with water, was used for thermal hydrolysis tests. Throughout the experiment, a proportional-integral—differential (PID) controller managed parameters such as gas flow, humidifier temperature, and reactor temperature. A backpressure controller was installed at the end of the gas line to regulate pressure. As a safety measure, both the reactor and humidifier were filled to 70% capacity. All the assays were carried out in the presence of nitrogen, with a gas flow of 2000 mL/min.

The operating pressure was maintained at 20 bar, and the temperature ranged from $120\,^{\circ}\text{C}$ to $150\,^{\circ}\text{C}$. This temperature range was chosen to achieve an optimal balance between biomolecule solubilization and particle size distribution, since higher temperatures result in the degradation of the biopolymers (García et al., 2017). In addition, at $120\,^{\circ}\text{C}$, residence times from 1 h to 4 h, and pH levels from 6.6 to $10\,^{\circ}$ were examined. After each reaction was completed, a sample was collected in a sterile container and centrifuged at 10,000g for $20\,^{\circ}$ min. The supernatant was cooled to room temperature and used to produce

BMHB. Besides, the supernatant was also employed for physicochemical characterization, heavy metal determination and microbiological analyses.

2.3. Sewage sludge analytical methods and microbiological assays

2.3.1. Physicochemical characterization of sewage sludge

Measurements of SCOD, TCOD, TSS, VSS and pH were carried out according to Standard Methods (APHA, 2012). Quantification of proteins and humic-like substances was conducted using the modified Lowry method (Lowry et al., 1951), with bovine serum albumin (BSA) and humic acid as standards, respectively. The Dubois method was applied to determine carbohydrate content using D-glucose as a standard (DuBois et al., 1956). All analyses were performed in triplicate, and the reported results represent the mean values.

2.3.2. Size exclusion chromatography analysis

To determine the molecular size distribution of the solubilized biopolymers (fingerprints), a high-performance liquid chromatography system (Agilent Technologies Inc., USA) was employed, utilizing a Thermo ScientificTM BioBasicTM SEC 300 column (4.6 mm × 300 mm). The mobile phase consisted of 0.1 M K₂HPO₄ buffer solution adjusted to pH 7 with a flow rate of 0.35 mL/min. UV diode array detectors at a wavelength of 280 nm were used in these analyses. A mixture of diverse proteins between 15 and 600 kDa were used as a standard calibration set (Sigma-Aldrich, 69385), including Ribonuclease A (13.7 kDa), Albumin (44.3 kDa), γ-Globulin (150 kDa) and Thyroglobulin (670 kDa), also including ρ-aminobenzoic acid (0.14 kDa) as a low molecular weight marker. The calibration curve exhibited a coefficient of determination (R²) of 0.99. The column volume was assessed using NaNO₃ solution, yielding 4.06 mL (11.59 min). Considering the direct influence of biomolecules size on BMHB properties (Zhong et al., 2019), the particles were divided into three classes: large (>150 kDa or < 8.22 min), medium (15–150 kDa or between $8.22 \, \text{min}$ and $10.36 \, \text{min}$) and small (<15 kDa or between 10.36 min and 11.59 min). Any signal detected beyond the end of the column were considered as molecules that interact with the column packing, reflecting a hydrophobic behavior (Guan et al., 2017; Simon et al., 2009). Prior to injection (20 µL), each sample was filtered through a Simplepure PVDF/L 0.45 μm filter.

2.3.3. Heavy metal determination

An ICP-MS Agilent $7700\times$ (Agilent Technologies Inc., USA), equipped with an integrated I-AS autosampler, was used to determine the concentrations of heavy metals (Hg, Cd, Cr, Pb, Ni, Cu, Zn and Al) in the samples. To remove interference, a flow of 4.3 mL/min of He was used in the collision/reaction cell. The standards used in the metal analysis were Sc (for Al, Cr, Ni, Cu and Zn), Rh (for Cd) and Ir (for Hg and Pb).

2.3.4. Microbial growth analysis

To analyze microbial growth in the hydrolyzed sewage sludges, 100 μ L of the undiluted supernatant was inoculated onto Plate Count Agar (PCA) medium. The inoculated plates were then incubated under aerobic conditions at 30 °C for 72 h. Duplicate samples were analyzed for each condition (Junaidi et al., 2022).

2.4. BMHB preparation

The supernatants from the hydrolyzed and centrifuged sewage sludges (obtained under different operating conditions) were frozen at $-80\,^{\circ}\text{C}$ for 12 h, and subsequently lyophilized at $-70\,^{\circ}\text{C}$ for 24 h using a Telstar Cryodos (Telstar Industrial S.L., Spain) at 0.1 bar pressure. Afterwards, 2.5 g of each of the freeze-dried sludge powders were dissolved in a mixture of 50 mL of water and glycerol (plasticizing agent) at a ratio of 0.3 g of glycerol/1 g of lyophilized hydrolyzed sludge powder. Silicone molds were used to shape the resulting BMHB solutions, which were then dried at 37 $^{\circ}\text{C}$ for 24 h.

L. Romero et al. Waste Management 174 (2024) 31-43

2.5. BMHB characterization

Before undergoing characterization, BMHB samples were equilibrated in a Memmert HCP50 humidity chamber (Memmert, Germany) at 25 °C under a controlled relative humidity of 30% for at least one day.

2.5.1. BMHB thickness

For measuring the thickness of BMHB samples, a digital micrometer (Mitutoyo C, Japan), with a precision of $\pm 1~\mu m$ was used. Five measurements were taken at different points across the entire BMHB sample, and the reported data represent the mean values. The thickness measurements were conducted prior to the other tests.

2.5.2. Light absorbance and transparency

The light barrier properties of the BMHB samples were determined using the method proposed by Alvarez et al. (2021). A Thermo ScientificGenesys 150 UV-visible Spectrophotometer (Thermo Fisher Scientific, USA) was used to measure the absorbance at wavelengths from 280 to 800 nm. An empty quartz cuvette served as the blank. The calculation of the transparency of the BMHB samples was based on Equation (1).

$$Transparency = A_{600}/x \tag{1}$$

where A_{600} is the absorbance at 600 nm of the BMHB samples, and x is the mean thickness (mm).

2.5.3. BMHB color

An UltraScan VIS spectrophotometer (HunterLab, USA) was used to determine the color characteristics of the BMHB samples, which were measured according to the L*, a*, b* system. A white standard plate with L*, a*, b* values of 97.12, -0.14 and 0.13, respectively, was used as the reference surface. Eqs. (2) and (3) were employed for calculating the White Index (WI) and Chroma, respectively.

$$WI = 100 - \sqrt{(100 - L^*)^2 + a^{*2} + b^{*2}}$$
 (2)

$$Chroma = \sqrt{a^{*2} + b^{*2}} \tag{3}$$

2.5.4. Mechanical properties

A TA.XT. plus Texture Analyzer (Texture Technologies, USA) was used to assess the mechanical properties of the BMHB samples, employing a 50 N load cell and a 5 mm diameter probe (P/5S). The tests were conducted with a piece of the BMHB samples measuring 15 mm \times 30 mm, which were placed between two plates attached to the testing device. The plates on the analyzer have a 10 mm hole through which the probe made contact with the piece of the BMHB samples at 1 mm/s speed, stretching it until rupture occurred. From the tests, the puncture strength (PS) and the puncture deformation (PD) were calculated using Equations (4) and (5), respectively.

$$PS = Fm/Th (4)$$

$$PD = (\sqrt{D^2 + R^2} - R)/R \tag{5}$$

where: Fm (N) is the maximum force applied before the rupture of BMHB samples; Th (mm) is the thickness of the BMHB samples; D (mm) is the distance the probe reaches before the rupture of the BMHB samples; and R (mm) is the radius of the orifice in the plate.

2.5.5. Water vapor permeability and solubility

A polyvinyl chloride cup was partially filled with distilled water and sealed with a circular piece of the BMHB samples that matched the diameter of the cup. Water surface was maintained at a 1 cm height below the BMHB samples, and their thickness were also measured. Additionally, visual inspection was conducted to exclude the BMHB samples with pinholes or breakages. Subsequently, the cups were

weighted and placed in desiccators. Weight loss was monitored every hour for a total of 8 h to determine the water vapor transmission rate (WVTR). The WVTR was calculated according to Equation (6), which involved plotting the weight loss against time.

$$WVTR = G/(t\hat{A} \cdot A) \tag{6}$$

where G/t represents the weight change in the cups per unit of time (g/h), and A (m²) the area of BMHB samples covering the cup diameters.

Water vapor permeability (WVP) can be calculated from the WVTR values by using Eq. (7):

$$WVP = (WVTR\hat{A} \cdot Th)/\Delta P \tag{7}$$

where ΔP (kPa) represents the difference in partial pressure between the two faces of the BMHB samples, and Th (mm) is the thickness of BMHB samples.

For the solubility tests, a 40 mm circumference of each of the BMHB samples was cut and immersed in 50 mL of buffer solutions at different pH values (5, 7 and 9) for 24 h on an orbital shaker with gentle stirring. The water was then filtered using a vacuum pump and Whatman No. 1 filter paper to recover the insolubilized portion of the BMHB samples. To determine the dry mater of the recovered BMHB samples, an HR80 halogen moisture analyzer (Mettler-Total, Switzerland) was used after subjecting the samples to 12 h at 105 $^{\circ}\text{C}$. Prior to immersion in water, the moisture content of each of the BMHB samples was determined using the same moisture analyzer. The obtained values were compared to assess the extent of dissolution of the BMHB samples.

2.5.6. Contact angle

A CAM 200 Optical Contact Angle Gauge (KSV Instruments Ltd., USA) was employed to measure contact angles, determining the surface wettability of the BMHB samples. These tests involved measuring the angle between the baseline and the point where the water droplet contacted the BMHB surface. Approximately 20 μL of deionized water was dispensed onto the BMHB samples using a syringe and contact angle values remained constant after 10 s. A high-resolution CCD camera was used to capture the water droplets on the surface of the BMHB samples. Measurements for each of the BMHB samples were performed in triplicate, providing mean values. The KSV CAM 200 software was used for data analysis.

2.5.7. Thermal stability

A thermogravimetric (TG) analysis was performed to the BMHB samples using a Mettler Toledo TGA/STDA851e (Mettler Toledo, USA) employing a nitrogen atmosphere at a flow rate of 50 mL/min. The temperature was ramped from room temperature to 700 $^{\circ}\text{C}$ at a heating rate of 10 $^{\circ}\text{C/min}.$

2.5.8. Fourier-transform infrared spectroscopy (FTIR)

An attenuated total reflectance accessory (ATR) was mounted in the sample compartment of the Varian 670-IR spectrometer (Agilent Technologies, USA) for the FTIR analysis. Spectra were acquired between 4000 and $600~{\rm cm}^{-1}$ in the medium IR range. A total of 16 scans were performed with a resolution of 4 cm $^{-1}$.

2.5.9. Scanning electron microscopy

A JSM-6610LV scanning electron microscope (JEOL, USA) was employed to examine the cross-sectional microstructure of the BMHB samples. For this purpose, dried pieces of each of the BMHB samples measuring 1 cm^2 were coated with a thin layer of gold to make them conductive. The magnification was set to $\times 500$ and $\times 4000$, and the voltage to 20 kV.

2.5.10. Statistical analysis

Data analysis was performed using an ANOVA test, and Fisher's test was used to determine significant differences between samples by

L. Romero et al. Waste Management 174 (2024) 31–43

calculating least significant differences (LSD). Statistical analyses were conducted using Statgraphics® V.15.2.06.

2.6. Application of BMHB as a pesticide container

The use of BMHB as a pesticide container for agricultural purposes is an interesting application, as it prevents direct contact between farmers and toxic substances. In this context, acetamiprid ($\geq 95.0~\%$ purity, purchased from Thermo Scientific) was selected as a model pesticide for packaging. Rectangular packages, approximately 1.5 \times 3 cm, and 1 \times 1.5 cm in size, were prepared using an Impulse Sealer PFS-400 thermo sealer to ensure a secure seal.

To evaluate the disintegration and solubilization of the packaging material, the bag was placed in distilled water under low continuous stirring (100 rpm) until complete dissolution. Considering the maximum acetamiprid application rate, a pesticide concentration of 125 mg/L was used (European Commission, 2016).

3. Results and discussion

3.1. Thermal hydrolysis of sewage sludge

3.1.1. Biomolecule solubilization by thermal hydrolysis

Thermal hydrolysis process increased the kinetic energy of the molecules in sewage sludge, leading to the disruption of EPS and microbial cells, and subsequently, the release of biomolecules (Xue et al., 2015). The generation of a high quantity of biomolecules is essential for obtaining the bio-based material from the hydrolyzed sludge and, consequently, for producing of the BMHB samples.

Firstly, regarding VSS evolution, the results obtained revealed that higher temperatures resulted in better yields of VSS reduction compared to longer residence times. Consequently, a 51% reduction of VSS was

achieved at 150 °C for 2 h, whereas this value was 41% at 120 °C for 4 h (Fig. S1 of the Supplementary material). Additionally, the use of alkaline pH also favored VSS decrease, even at lower temperatures, where a 60% reduction was reached at 120 °C for 2 h with a pH of 10.

The organic matter solubilization in the sewage sludge led to an increased concentration of soluble biopolymers. Fig. 1 a, d and g shows the evolution of biopolymer concentration (proteins, humic-like substances, and carbohydrates), as a function of residence time, process temperature and pH, respectively. Across all treatment conditions, the results indicated a high degree of biopolymer solubilization, particularly proteins, followed by humic-like substances and carbohydrates. According to Urrea et al. (2017a), proteins are predominantly present in the intracellular material, which are released into the liquid phase when the temperature exceeds 100 °C due to the loss of cell membrane integrity. Meanwhile, humic-like substances constitute an essential part of sewage sludge EPS, which acts as a hydrated matrix resembling a three-dimensional gel (Simon et al., 2009). Finally, carbohydrates represent the least abundant biopolymer in sewage sludge. These create complex networks that adhere to the cell wall, thereby increasing their soluble concentration with increased process temperature or residence time (Seviour et al., 2019).

It is important to emphasize that the concentration of proteins and humic-like substances significantly increased when the medium pH was 10. Specifically, the values were 1.6 and 2.1 times higher than those obtained at neutral pH for proteins ($5033 \pm 13 \text{ mg/L}$; 185 mg/gVSS_0), and humic-like substances ($1873 \pm 55 \text{ mg/L}$; 49 mg/gVSS_0) under the same residence time (2 h) and temperature ($120 \, ^{\circ}\text{C}$). This difference is attributed to the dissociation of acid groups and repulsion of negatively charged moieties in EPS, which resulted in an increase in biomolecule concentration (Kang et al., 2011). Additionally, previous studies have suggested that alkaline media enhance the concentration of humic-like substances and proteins in the liquid media (García et al., 2020; Song

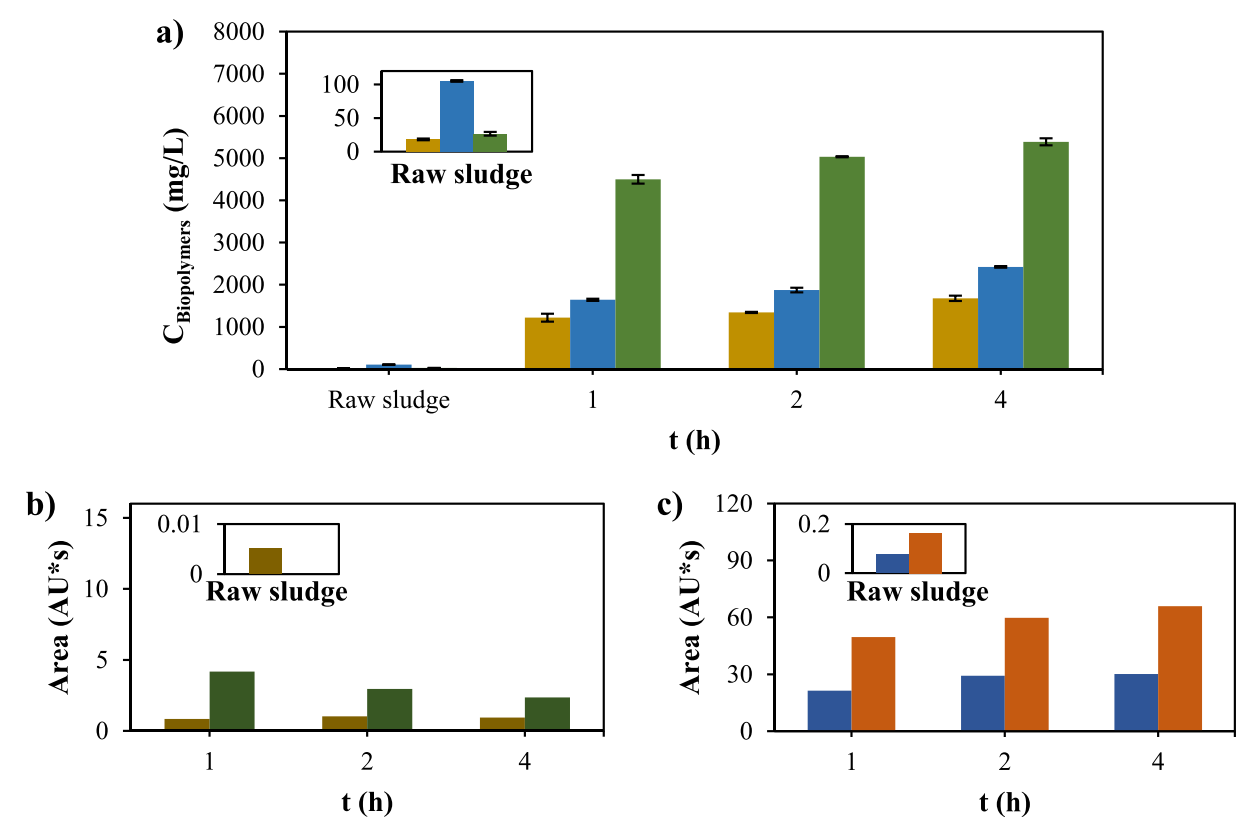


Fig. 1. Concentration of the solubilized biopolymers: proteins (■), humic-like substances (■) and carbohydrates (■), and fingerprints of the solubilized biopolymers at different sizes: >150 kDa (■), 15–150 kDa (■), <15 kDa (■) and hydrophobic-like behavior compounds (■), at different thermal hydrolysis operating conditions: (a–c) residence time (at 120 °C), (d–f) process temperature (for 2 h) and (g–i) pH (at 120 °C for 2 h). In all cases, pressure = 20 bar.

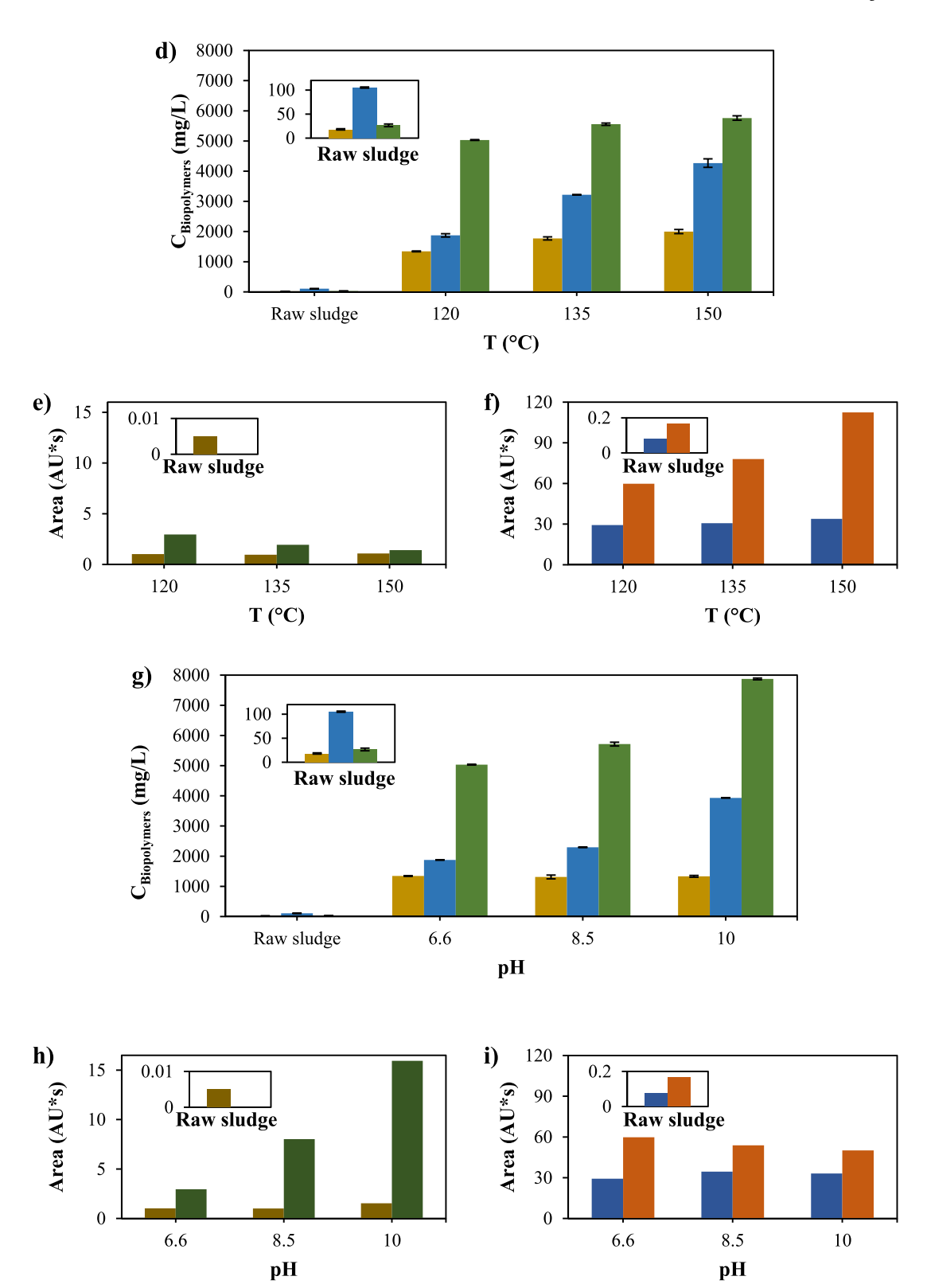


Fig. 1. (continued).

et al., 2019). This phenomenon may also account for the considerable VSS reduction observed when thermal-alkaline process was used, as indicated above. However, the increase in pH did not impact the concentration of carbohydrates during the thermal hydrolysis process. Similar behavior was reported by Ruiz-Hernando et al. (2015) when

sewage sludge was subjected to alkaline pH for 24 h, as they observed no significant changes compared to the hydrothermal treatment.

3.1.2. Biopolymer molecular size distribution (fingerprints)

In the preceding section, different key parameters in thermal

hydrolysis were carefully examined to assess their impact on the biomolecule solubilization. Nevertheless, it is also essential to determine the size distribution of these biomolecules in order to evaluate their possible impact on the formation and characteristics of the BMHB samples. Consequently, Fig. 1 b, c, e, f, h and i illustrates the distribution of the solubilized biomolecule fingerprints considering residence time, temperature process and pH value as well.

The impact of thermal hydrolysis is evident in the release of a substantial quantity of large and medium-sized molecules. While there were no significant changes in the large-sized molecules (>150 kDa) as the temperature or residence time increased, the medium-sized molecules (15-150 kDa) exhibited degradation. Specifically, a decrease of 52% was observed when the temperature increased from 120 °C to 150 °C for 2 h (from 2.95 to 1.41 AU*s); and a 44% decrease when the temperature was 120 °C and residence time increased from 1 h to 4 h (from 4.18 to 2.35 AU*s). Conversely, the small-sized molecules (<15 kDa) experience a 16% increase when the temperature raised from 120 $^{\circ}$ C to 150 $^{\circ}$ C for 2 h (from 29.26 to 33.88 AU*s); and a 41% increase when the temperature was 120 °C and residence time increased from 1 h to 4 h (from 21.39 to 30.16 AU*s). This observed increase in the smaller molecules can be linked to the breakdown of medium-sized molecules (Romero et al., 2023). Finally, in the case of hydrophobic polymers, the rise in their concentration at higher residence times (33%) and temperatures (88%) can partially be attributed to an increase in protein concentration, as proteins tend to exhibit hydrophobic behavior (Urrea et al., 2016). Regarding pH values, they also exerted a significant influence on the size distribution. In this sense, when the pH was set to 10, the values of large-, medium- and small-sized molecules were 1.5, 5.4 and 1.1 times higher, respectively, than those achieved at pH 6.6 for large- (1.02 AU*s), medium-(2.95 AU*s) and small-sized (29.2 AU*s) molecules, respectively. On viewing the results, alkaline thermal hydrolysis caused the soluble biomolecules to exhibit a more hydrophilic behavior. This phenomenon can be attributed to the repulsion of negatively charged EPS induced by

the alkaline pH. Furthermore, this effect could also explain why the polymers with hydrophobic behavior decreased by 16% compared to neutral pH (59.7 AU*s).

3.1.3. Analysis of microbial growth and heavy metal content in hydrolyzed sewage sludge

The sludge generated by sewage treatment plants contains elevated levels of pathogens and hazardous materials, including heavy metals. It is crucial that these do not exceed regulated limits if the sewage sludge is used for agricultural purposes (González-Tolivia et al., 2022).

Microbial growth in the liquid phase of the hydrolyzed sludge was analyzed to ensure the absence of microorganism development on the BMHB samples. Additionally, the presence of heavy metals was investigated to assess if any were dissolved during thermal hydrolysis and could potentially be transferred to the BMHB samples. Measurements of heavy metals were taken in the lyophilized powder of the hydrolyzed sludges before preparing the BMHB-forming solution. Fig. 2 shows that no microorganism growth occurred after 72 h of incubation at temperatures of 120 °C and 135 °C, residences times from 1 h to 4 h and pH values from neutral to alkaline. These results are consistent with those reported by Guo et al. (2008), who sterilized sewage sludge at 121 °C for 15 min. It should be noted that due to the absence of microbial growth in the samples at 120 °C and 135 °C; 2 h, no further analysis was conducted for the sample at 150 °C for 2 h.

With regard to the heavy metal content in the hydrolyzed sewage sludges, Table S2 (Supplementary material) shows the permissible limits for heavy metal concentrations according to Spanish legislation (Agricultura and Alimentación, 1990). These limits are provided based on soil pH. Additionally, the concentrations measured in the lyophilized powder of the hydrolyzed sewage sludge under different operating conditions are also presented. It should be noted that none of the heavy metals (Hg, Cd, Cr, Pb, Ni, Cu, Zn and Al) found in lyophilized sewage sludge powder exceeded the limits set by legislation. Consequently, the BMHB

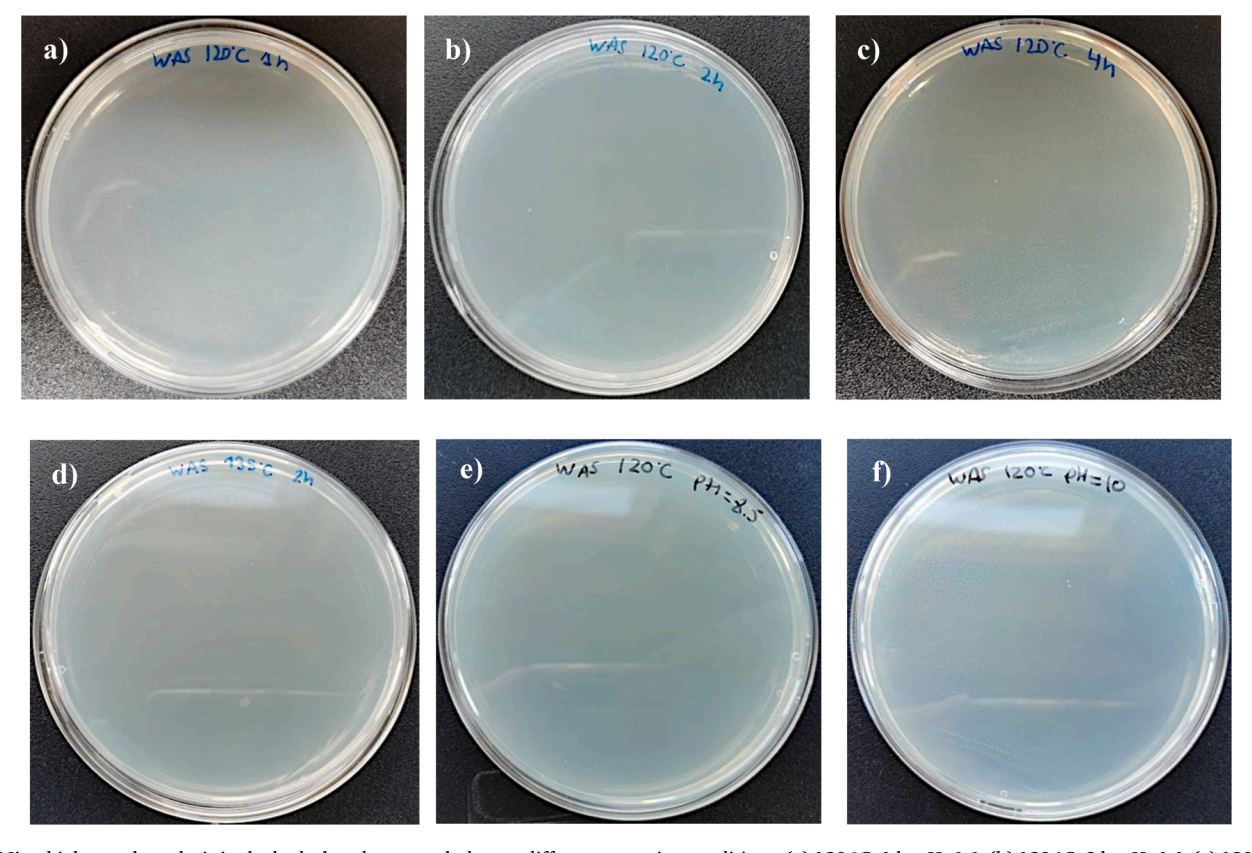


Fig. 2. Microbial growth analysis in the hydrolyzed sewage sludges at different operating conditions: (a) 120 °C, 1 h, pH: 6.6; (b) 120 °C, 2 h, pH: 6.6; (c) 120 °C, 4 h, pH: 6.6; (d) 135 °C, 2 h, pH: 6.6; (e) 120 °C, 2 h, pH: 8.5 and (f) 120 °C, 4 h, pH: 10.

samples can be employed for agricultural applications. Additionally, the results indicated a slightly increase in the content of Cr, Pb, Ni, Cu and Zn under alkaline conditions, with the exception of Al, which exhibited a significant increase. This trend can be attributed to the aforementioned phenomenon wherein negative charges repel at basic pH, leading to the release of various compounds, including heavy metals. Initially, these metals are bioabsorbed into the EPS matrix through complexation with negatively charged functional groups (Pola et al., 2021).

3.2. BMHB properties

3.2.1. Visual appearance, light absorbance, transparency, and color evaluation

Fig. 3 shows the visual appearance of the prepared BMHB samples. After 24 h of equilibration in the humidity chamber, most samples were easily removed from the silicone mold. However, exceptions were observed for the BMHB samples prepared from hydrolyzed sewage sludge at 135 °C for 2 h, and pH: 6.6, as well as 150 °C for 2 h, and pH: 6.6. Due to their sticky and unwieldy texture, these samples were excluded from further characterization. This can be attributed to the excessive biomolecule breakdown at higher temperatures, which amplified the lubricating effect of glycerin, as it interacts within the spaces between polymer chains, increasing the water diffusion and causing heightened slippage when there are more, but smaller, molecules (Ben et al., 2022; Gao et al., 2023). Each of the BMHB samples was assigned a number from 1 to 5, which will be further used for easier identification.

Table 1 presents color, light absorbance and transparency values of the BMHB samples obtained from hydrolyzed sewage sludge at different operating conditions. The L^* values, which signify brightness (with higher values indicating greater brightness and lower values indicating darkness), exhibited statistically significant differences (p < 0.05).

However, there were no statistically significant differences observed in the case of a* values (positive values indicating redness and negative values indicating greenness) and b* values (positive values indicating yellowness and negative values indicating blueness). Collectively, these values are characteristic of a dark color with a warm undertone that tends towards reddish and yellowish hues.

Regarding chroma values, they varied from 15.2 \pm 0.9 to 19 \pm 1, indicating a spectrum of saturated and vivid colors. Interestingly, no significant differences were observed among all the tested BMHB samples in terms of chroma values, which was consistent with the trends observed in a* and b* values. This suggests that the saturation and vibrancy of color remained relatively consistent across the tested BMHB samples.

The WI parameter, which evaluates the lightness or darkness of the BMHB samples relative to a white standard plate, consistently showed low values across all cases, with values up to 17.2 \pm 0.4, indicating dark or highly saturated colors. Notably, when the pH was set at 10, the WI value was particularly low (5.2 \pm 0.2). This low WI value exhibited significant differences when compared to BMHB 1-3 but no significant differences when compared to BMHB 4, aligning with the observed trends in L* values. This consistency in results corresponded with the dark brown coloration observed in all BMHB samples. This distinctive coloration is typically associated with the presence of quinones and phenolic compounds released during the thermal hydrolysis of sewage sludge, as previously reported (Urrea et al., 2017b). Furthermore, the heightened presence of humic-like substances contributed to this coloration due to their predominant composition of carboxylic and phenolic groups (García et al., 2020). As previously mentioned, alkaline thermal hydrolysis facilitated the solubilization of sludge flocs. This resulted in a higher concentration of color-rising compounds in the hydrolyzed sludge, leading to the observed reduction in WI for BMHB 4 and 5.

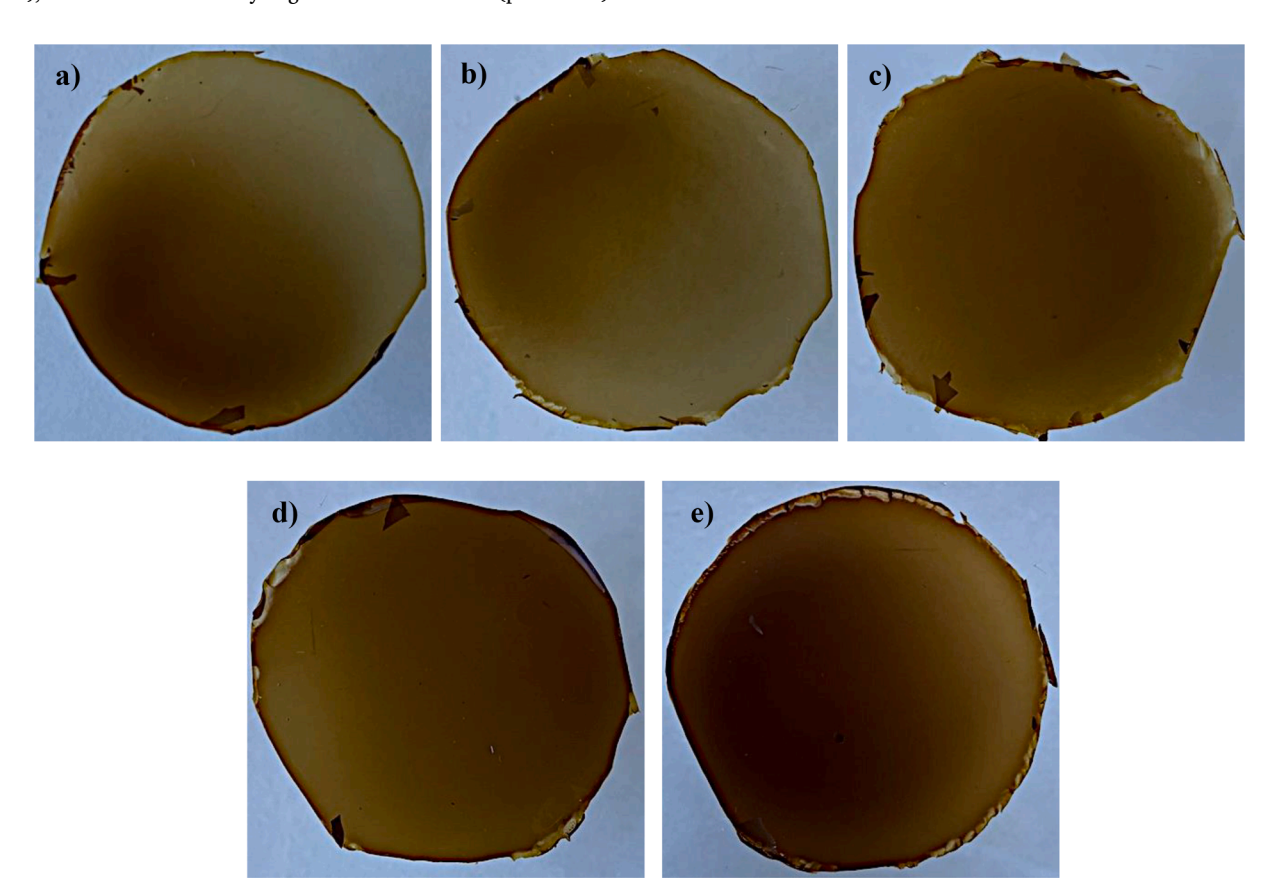


Fig. 3. Visual appearance of the BMHB samples obtained from hydrolyzed sewage sludges at different operating conditions. (a) BMHB 1: 120 °C, 1 h, pH: 6.6; (b) BMHB 2: 120 °C, 2 h, pH: 6.6; (c) BMHB 3: 120 °C, 4 h, pH: 6.6; (d) BMHB 4: 120 °C, 2 h, pH: 8.5 and (e) BMHB 5: 120 °C, 2 h, pH: 10.

Table 1Color, light absorbance and transparency of the BMHB samples.

$Sample^{(1)}$	Thickness (mm)		Color							
			L*		a*	b*	Whit	e Index, WI	Chroma	
ВМНВ 1	$0.19\pm0.05^{\rm a}$		$16.5\pm0.7^{\rm a}$		13.0 ± 0.4^a	11.8 ± 0.6^{a}	14.7	$\pm 0.6^a$	17.6 ± 0.6^{a}	
BMHB 2	0.181 ± 0.006^{a}		16.7 ± 0.4^{a}		14.23 ± 0.07^{a}	9.0 ± 0.1^a	15.0	$\pm~0.8^a$	16.7 ± 0.3^{a}	
ВМНВ 3	0.18 ± 0.03^{a}		19 ± 2^a		12.27 ± 0.07^{a}	9.0 ± 0.6^a	17.2	$\pm~0.4^a$	15.2 ± 0.9^{a}	
BMHB 4	0.19 ± 0.01^a		13.0 ± 0.2^{ab}		15.3 ± 0.6^a	9.4 ± 0.6^a	11.2	$\pm~0.1^{ab}$	17.5 ± 0.4^{a}	
BMHB 5	0.2 ± 0.01^a		$\textbf{7.2} \pm 0.1^{\text{b}}$		18 ± 2^a	6.7 ± 0.2^a $5.2 \pm$		± 0.2 ^b	19 ± 1^a	
Sample	Light absorbance (Wavelength, nm)									
	280	300	350	400	500	600	700	800		
BMHB 1	4.9±0.2 ^a	4.8±0.3 ^a	4.7±0.5 ^a	4±1 ^a	1.4±0.5 ^a	0.7±0.2 ^a	0.4±0.1 ^a	0.23±0.05 ^a	3.75±0.08 ^b	
BMHB 2	$4.9{\pm}0.2^{a}$	4.9 ± 0.2^{a}	4.7 ± 0.5^{a}	$3.7{\pm}0.4^{a}$	1.36 ± 0.06^{a}	$0.69{\pm}0.06^{a}$	0.41 ± 0.08^{a}	$0.27{\pm}0.05^{a}$	$3.7{\pm}0.2^{\mathrm{b}}$	
вмнв з	5 ± 0^a	5 ± 0^a	5 ± 0^a	$4.5{\pm}0.9^{a}$	$1.8{\pm}0.4^{a}$	$0.9{\pm}0.2^{a}$	$0.5{\pm}0.1^{a}$	$0.3{\pm}0.1^{a}$	$3.4{\pm}0.2^{\mathrm{b}}$	
BMHB 4	5 ± 0^a	5 ± 0^a	5 ± 0^a	$4.4{\pm}0.2^{a}$	$1.49{\pm}0.07^{a}$	$0.69{\pm}0.03^{a}$	$0.35{\pm}0.02^a$	$0.19{\pm}0.01^a$	$3.9{\pm}0.2^{\rm b}$	
BMHB 5	5 ± 0^a	5 ± 0^a	5 ± 0^a	$4.9{\pm}0.2^{a}$	$2.0{\pm}0.2^a$	$0.97{\pm}0.04^{a}$	$0.47{\pm}0.05^a$	$0.27{\pm}0.04^{a}$	5.01 ± 0.05^{a}	

Different letters in the same column indicate significant differences (P < 0.05).

Each number refers to the BMBH samples obtained from hydrolyzed sewage sludges at different operating conditions: BMHB 1: 120 °C, 1 h, pH: 6.6; BMHB 2: 120 °C, 2 h, pH: 6.6; BMHB 3: 120 °C, 4 h, pH: 6.6; BMHB 4: 120 °C, 2 h, pH: 8.5 and BMHB 5: 120 °C, 2 h, pH: 10.

An important point to emphasize is the high absorbance of ultraviolet light (280–400 nm) observed in all the tested BMHB samples (Sankaran and Ehsani, 2014). This absorption is due to the interaction of carbonyl groups within peptide bonds, aromatic amino acids present in the protein primary structure, and disulfide bonds (Alvarez et al., 2021). This property proves to be beneficial for the applications of BMHB, which acts as a barrier against light exposure (Pirsa et al., 2020), thereby hindering oxidative degradation caused by UV radiation. Transparency values were also quite elevated in all cases, further proving the suitability of the BMHB samples. Based on the results of visible light absorbance, it can be deduced that the BMHB samples tends to exhibit a translucent aspect. Thus, the absorbance values in the range 600—800 nm varied from 0.19 \pm 0.01 to 0.9 \pm 0.2, with an exception at 500 nm (Guzman-Puyol et al., 2022).

3.2.2. Mechanical properties

The structural integrity of BMHB is essential as they undergo shipping, handling, and storage, subjecting the materials to various stresses. In this regard, an assessment of the mechanical properties of the BMHB samples was conducted (Table 2). Notably, both PS and PD showed significantly higher values at basic pH levels compared to neutral conditions, with significant differences (p < 0.05). Specifically, at pH 10, the PS and PD values were approximately 1.4 and 2.1 times higher than those obtained at neutral pH (PS = 45 \pm 4 N/mm; PD = 13 \pm 1%). This trend can be attributed to the molecular size distribution, as large- and

Table 2Puncture strength (PS), puncture deformation (PD), water vapor permeability (WVP) and solubility of the BMHB samples.

Sample ⁽¹⁾	PS (N/ mm)	PD (%)	WVP (g*mm/ m ² *h*kPa)	Solubilit pH 5.0	y (%) pH 7.0	pH 9.0
ВМНВ 1	$^{46~\pm}_{3^b}$	$\begin{array}{c} 15.9 \pm \\ 0.8^{bc} \end{array}$	3.9 ± 0.1^a	$\begin{array}{l} 95.3 \\ \pm \ 0.7^a \end{array}$	96 ± 1 ^a	$93.0 \\ \pm 0.9^a$
вмнв 2	$\begin{array}{l} 45\ \pm \\ 4^b \end{array}$	13 ± 1^{c}	4.0 ± 0.3^a	$95.6 \\ \pm 0.2^a$	94 ± 1^a	$\begin{array}{c} 94 \; \pm \\ 1^a \end{array}$
вмнв 3	$\begin{array}{c} 44\ \pm \\ 2^b \end{array}$	12 ± 2^{c}	4.2 ± 0.4^a	$\begin{array}{l} 96.1 \\ \pm \ 0.8^a \end{array}$	$\begin{array}{c} 93 \; \pm \\ 2^a \end{array}$	$\begin{array}{c} 95 \ \pm \\ 3^a \end{array}$
ВМНВ 4	$58 + 6^{a}$	$\begin{array}{c} 20.3 \; \pm \\ 0.7^b \end{array}$	3.7 ± 0.1^a	$\begin{array}{l} 94.2 \\ \pm \ 0.9^a \end{array}$	96 ± 0.7^{a}	95 ± 3 ^a
ВМНВ 5	$63.7 \\ \pm 0.2^a$	$\begin{array}{c} 27.8 \pm \\ 0.9^a \end{array}$	3.5 ± 0.3^a	$\begin{array}{c} 90 \ \pm \\ 2^a \end{array}$	95 ± 2^a	$\begin{array}{l} 93.1 \\ \pm \ 0.3^a \end{array}$

Different letters in the same column indicate significant differences (P < 0.05). $^{(1)}$ Each number refers to the BMBH samples obtained from hydrolyzed sewage sludges at different operating conditions: BMHB 1: 120 °C, 1 h, pH: 6.6; BMHB 2: 120 °C, 2 h, pH: 6.6; BMHB 3: 120 °C, 4 h, pH: 6.6; BMHB 4: 120 °C, 2 h, pH: 8.5 and BMHB 5: 120 °C, 2 h, pH: 10.

medium-sized molecules increased significantly at alkaline pH levels. This finding aligns with that found by Zhong et al. (2019), who reported that chitosan-based films exhibited enhanced mechanical strength with higher molecular weights, attributed to improved polymer structure and self-aggregation. In addition, protein-based materials are characterized by having good mechanical resistance (Calva-Estrada et al., 2019). Thus, thermal hydrolysis at alkaline pH resulted in a higher yield of solubilized proteins (289 mg/gVSS $_0$ for 2 h at pH 10) in comparison to neutral pH conditions, even over an extended residence time (198 mg/gVSS $_0$ for 4 h at pH 6.6).

The PS values of the BMHB samples were similar to those reported by other authors. For instance, Jakob et al. (2002) obtained an average PS value of 44 \pm 5 N/mm for a material made up of layers of paper, aluminum, and high-density polyethylene, showing nearly identical values to those obtained from samples at neutral pH. Similarly, they reported a PS value of 61 \pm 4 N/mm for a material based on layers of paper, aluminum, and polyvinylidene chloride, closely aligning with the values obtained for the samples at alkaline pH.

3.2.3. Water vapor permeability and solubility

As shown in Table 2, the WVP values of the BMHB samples exhibited no significant differences (p < 0.05), with values ranging from 3.5 ± 0.2 g*mm/m²*h*kPa to 4.2 ± 0.4 g*mm/m²*h*kPa. It should be noted that these values are 2.3 to 4.1 times lower than those obtained from other protein-based materials, including dried distiller grains (8.86 \pm 0.04 g*mm/m²*h*kPa, (Yang et al., 2016)), chicken feather protein/nanoclay composite (11.2 \pm 0.6 g*mm/m²*h*kPa, (Song et al., 2013), and pea protein isolate (15.7 \pm 0.5 g*mm/m²*h*kPa, (Gao et al., 2023)). Therefore, these values can be considered moderately low, making BMHB suitable as a moisture barrier, preventing its introduction. This is particularly beneficial for packaging hazardous compounds to maintain their quality and properties.

Concerning the solubility of the BMHB samples, very high values were obtained (ranging from 90 \pm 2 to 96.1 \pm 0.8), with no significant differences (p < 0.05) regardless of the buffer solutions (Table 2). These elevated values make the BMHB samples an ideal choice for packaging hazardous compounds that need to be dissolved in water without requiring human handling.

Furthermore, it important to highlight a key advantage the of this approach: the use of the BMHB samples can significantly contribute to the reduction of discarded packaging materials, thereby promoting ecofriendly packaging solutions.

3.2.4. Thermal stability and wettability

A TG analysis was conducted to assess the thermal stability of the

BMHB samples. Fig. 4a illustrates the thermal decomposition curves of these samples obtained under different thermal hydrolysis conditions. Consistent behavior was observed across all BMHB samples, identifying three different stages of thermal degradation. The first stage was observed at temperatures from 25 °C to 125–150 °C, mainly attributed to the loss of interstitial and free water. During this phase, approximately $8 \pm 1\%$ of the total BMHB weight was lost.

The second stage took place within the temperature range of 150–400 °C. At this point, the material likely underwent decomposing due to the loss of glycerin (190–250 °C), cleavage of glycosidic bonds (140–310 °C), breakdown of low volatility molecules, and thermal protein degradation (270–280 °C) (Charles et al., 2022; Giovanela et al., 2004; Marcet et al., 2017; Nordin et al., 2020). The BMHB samples experienced a weight loss of 61.7 \pm 0.5% during this stage.

Finally, a third degradation stage occurred at temperatures between 400 and 700 $^{\circ}$ C, during which carbon converted into gaseous products of lower molecular weight. At this point, the material reached a final degradation of 74.0 \pm 0.9%, attributing the remaining final weight to minerals and carbonized residues (Celebi and Kurt, 2015). These results indicate that the BMHB samples remained stable up to 150 $^{\circ}$ C, highlighting their applicability not only at room or low temperatures but also at moderately elevated temperatures.

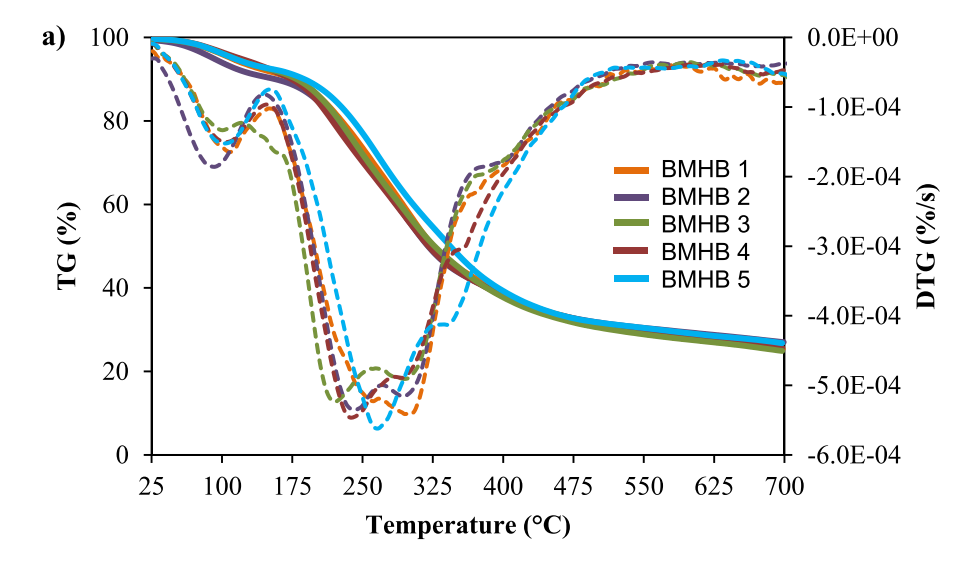
Contact angle measurements were performed to evaluate the

wettability of the BMHB samples, which characterizes the interaction between the solid material and a liquid (in this case, water). On viewing Fig. 4 b-f, all samples exhibited high wettability or hydrophilicity, as their contact angles were below 90° (Bracco and Holst, 2013). Notably, a slight increase in contact angles was observed in the BMHB samples derived from alkaline hydrolyzed sludge (BMHB 5 and BMHB 6). This phenomenon can be attributed to the predominance of the medium-sized molecules (15–150 kDa). As explained previously, an increased quantity of medium-sized molecules inhibited glycerin access into the biomolecular network, consequently impeding water diffusion (Gao et al., 2023).

3.2.5. FTIR spectra

FTIR spectra of the BMHB samples and glycerol are shown in Fig. S2 of the supplementary material. Regarding glycerol, the IR bands were located at 3271 cm⁻¹ (O–H stretching vibration), 2931 cm⁻¹ (C–H stretching vibration), 1412 cm⁻¹ and 1326 cm⁻¹ (related to with C–H bending vibration), 1107 cm⁻¹ (related to C–C group stretching vibration), 1028 cm⁻¹ and 992 cm⁻¹ (both related to C–O group stretching vibration), 920 cm⁻¹ and 850 cm⁻¹ (related to the torsion vibration of the –CH₂ group and the stretching vibration of the C–O–C group, respectively) (Fuertes et al., 2017; Ishak et al., 2016; Socrates, 2003).

Considering the BMHB samples, similar infrared bands were





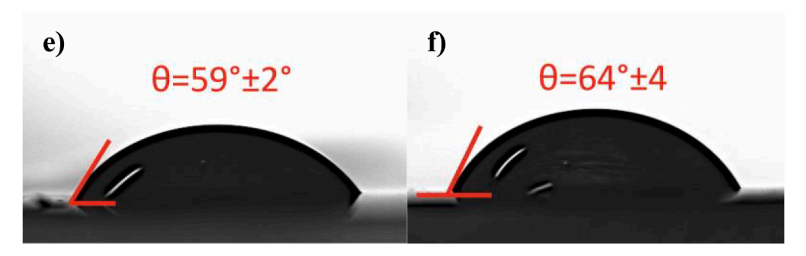


Fig. 4. (a) TG (percentage of weight loss, in solid lines) and dtg (derivative of weight loss, in dashed lines) of the bmhb samples. images of sessile droplets and contact angle values on the bmhb samples obtained from hydrolyzed sewage sludges at different operating conditions: (b) bmhb 1: 120 °C, 1 h, pH: 6.6; (c) BMHB 2: 120 °C, 2 h, pH: 6.6; (d) BMHB 3: 120 °C, 4 h, pH: 6.6; (e) BMHB 4: 120 °C, 2 h, pH: 8.5 and (f) BMHB 5: 120 °C, 2 h, pH: 10.

L. Romero et al. Waste Management 174 (2024) 31-43

observed in all cases. The band located at \sim 3267 cm $^{-1}$ can be attributed to the presence of both glycerol and proteins. In the case of proteins, it is assigned to the N-H stretching and hydrogen bonding of the amide A group (Fuertes et al., 2017). However, a slight shift to a lower value was observed compared with the isolated glycerol, which is due to the fact that the N-H peptide groups involved in hydrogen bonds changed position to lower frequencies (Nagarajan et al., 2012). The bands observed between 2864 and 2883 cm⁻¹ were assigned to C-H stretching, which are generally related to the presence of aliphatic chains (Grube et al., 2006). The peaks between 1622 and 1630 cm⁻¹ can be attributed to amide I bands and are commonly observed for the secondary protein structure β -sheet type. The observed peaks in the range 1513–1535 cm⁻¹ are due to a weak shoulder band of amide II. In this sense, the bands from 1513 to 1519 cm⁻¹ are linked to an antiparallel β -sheet structure, while those at 1535 cm⁻¹ are related to a parallel β -sheet structure (Pelton and McLean, 2000). According to Crichton (2008), an antiparallel structure offers greater stability in its hydrogen bonds due to the direction of these, making for stronger and more solid bonds. The bands around ~1400 and ~1230 cm⁻¹ are linked to carboxylate groups and C-O sections in carboxylic acids, respectively, being functional groups present in humic-type substances (García et al., 2020; van Veenhuyzen et al., 2021). There is a broad band around 1032 cm⁻¹ in all samples, which could be attributed to Si-O vibrations arising from silicate impurities, potentially in conjunction with clay minerals forming complexes with humic acids, as well as C-O stretching vibrations within polysaccharides or analogous polysaccharide-based compounds (Grube et al., 2006). Finally, the peaks observed at \sim 921 and \sim 850 cm⁻¹ are linked to the -CH₂ and C-O-C functional groups of glycerol.

3.2.6. Scanning electron microscopy (SEM)

Fig. 5 provides valuable insights into the microstructural characteristics of the BMHB samples. The examination of these micrographs reveals distinct differences among the various BMHB samples, which can be correlated to their mechanical properties.

Tiny holes or voids are present within the microstructure in BMHB 1, 2, and 3. These voids are more pronounced in BMHB 3, indicating a less compact and somewhat porous structure in this particular sample. These observations align with the trends observed in the mechanical properties of the BMHB samples, specifically the lower mechanical performance in BMHB 1, 2, and 3.

Conversely, the microstructure of BMHB 4 and BMHB 5 exhibits a distinct contrast, appearing smoother and more uniform. This characteristic is particularly noticeable in BMHB 5. This uniformity in microestructure suggests a denser and more structurally consistent material, which is in line with the enhanced mechanical properties observed in BMHB 4 and 5. The correlation between microstructure and mechanical properties is influenced by the sewage sludge processing conditions selected, particularly the use of alkaline hydrolysis. This treatment led to a higher presence of larger molecules in the solubilized biopolymers, which contributed to the denser microstructure and improved mechanical performance (Zhong et al., 2019).

3.3. Application of BMHB as a pesticide container

BMHB holds significant promise as a pesticide container primarily due to its favorable mechanical, wettability, and light absorbance characteristics. As illustrate in Fig. 6a, acetamiprid, a highly toxic compound requiring careful handling (Phogat et al., 2022), was contained within the BMHB 5 sample prepared from the alkaline hydrolyzed sludge. This selection was based on its superior mechanical properties.

Fig. 6b shows that the bag ruptured within 5 min of immersion in water, rapidly releasing the pesticide. Approximately 20 min after starting the test, the bag had nearly dissolved, remaining only 5% of the BMHB residues in the final solution. This rapid degradation can be attributed to the remarkable hydrophilicity and solubility of this biobased material. Importantly, when applied in soil, this material is deemed safe, thanks to the absence of microorganisms and its compliance with legal standards regarding heavy metal content. Furthermore,

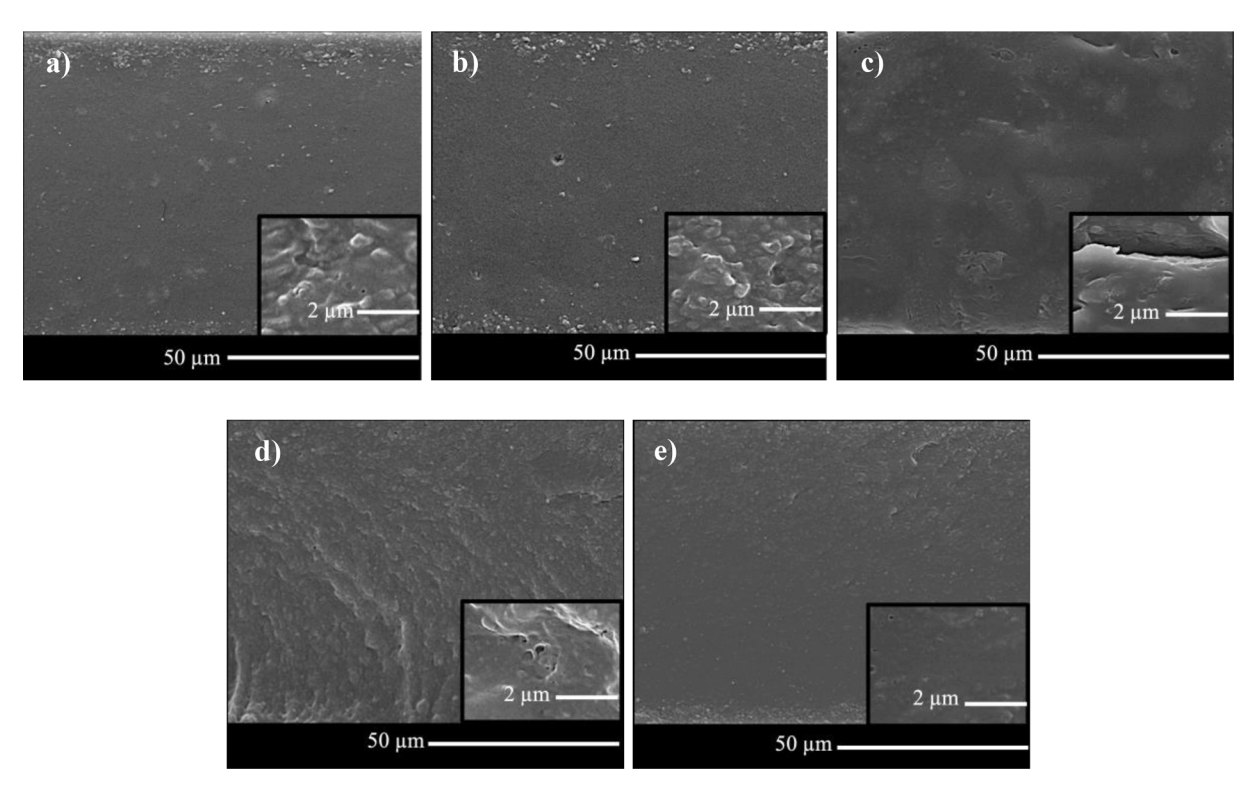
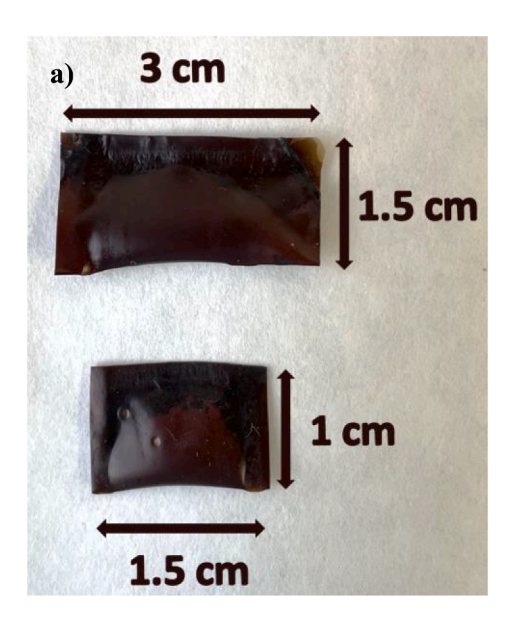


Fig. 5. Cross-sectional micrographs, with a magnification of \times 500 in the main micrographs and \times 4000 in the detailed micrographs, of the BMHB samples obtained from hydrolyzed sewage sludges at different operating conditions: (a) BMHB 1: 120 °C, 1 h, pH: 6.6; (b) BMHB 2: 120 °C, 2 h, pH: 6.6; (c) BMHB 3: 120 °C, 4 h, pH: 6.6; (d) BMHB 4: 120 °C, 2 h, pH: 8.5 and (e) BMHB 5: 120 °C, 2 h, pH: 10.



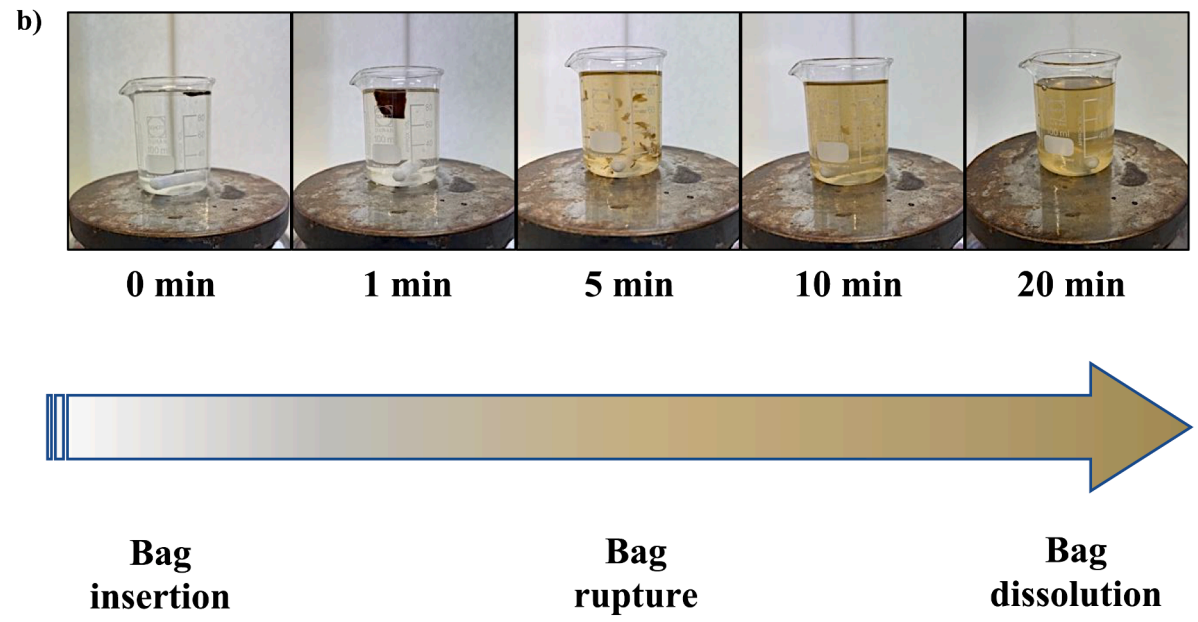


Fig. 6. (a) Picture of the bmhb 5 sample (obtained from hydrolyzed sewage sludge at 120 °C, 2 h, pH: 10) containing acetamiprid. (b) Water solubilization of the BMHB 5 sample containing acetamiprid.

the presence of proteins and humic-like compounds within BMHB enhances its suitability for soil applications by potentially serving as fertilizers, thereby enriching the nutrient content of the substrate, as highlighted by García et al. (2017).

Moreover, the material serves as a UV light barrier, thereby preserving acetamiprid effectiveness. UV light has a detrimental impact on its efficacy, as proved by Gupta et al. (2008), who reported over 90% dissipation after 24 h of exposure. Additionally, this packing composed of hydrolyzed sewage sludge and glycerin, can be considered biodegradable and eco-friendly (Ben et al., 2022; Pola et al., 2022), thus opening a novel pathway for the valorization of sewage sludge in the production of high-value added products, aligning with the pursuit of sustainable development objectives.

Finally, a preliminary evaluation of the costs associated with the obtention of BMHB from sewage sludge can be found Section S1 and Fig. S3 in the Supplementary material. Thus, the production cost of BMHB from 1 kg of sewage sludge amounts to ϵ 4.35, equivalent to ϵ 0.11

per gram of BMHB. It should be noted that the lyophilization stage was the most cost-intensive operation within the entire process, constituting 81% of the overall costs. This operation was selected to preserve the integrity of compounds in hydrolyzed sewage sludge, avoiding the loss of essential constituents, and protected it from chemical reactions that can occur during process like liquid water extraction or vaporization (Mellor and Bell, 1993). Nevertheless, in the context of scaling up this procedure, it becomes crucial to explore more cost-effective approaches for removing water from hydrolyzed sewage sludge.

4. Conclusions

Sewage sludge can be considered a potential bio-based material to produce hermetic bags (BMHB). Thermal hydrolysis conditions (temperature, residence time and pH) significantly affected both the concentration of solubilized biopolymers: proteins, humic-like substances and carbohydrates, and their molecular size. Additionally, these

L. Romero et al. Waste Management 174 (2024) 31-43

conditions exerted an important influence on the resulting texture of the BMHB. Specifically, samples derived from sewage sludge hydrolyzed at high temperatures (135 °C and 150 °C) exhibited a sticky and unwieldy nature. In contrast, the most favorable results were obtained under high alkaline conditions (pH 10), characterized by elevated concentration of proteins (7873 \pm 29 mg/L) and humic-like substances (3931 \pm 151 mg/L), an increased presence of large- (1.53 AU*s) and medium-sized molecules (15.94 AU*s), and reduced levels of hydrophobic compounds (50.09 AU*s).

The characterization of the BMHB samples indicated their potential as a barrier against light exposure, thus hindering oxidative degradation caused by UV radiation. Additionally, the absence of microorganisms and the compliance of heavy metal content with regulations underscored their safety. Moreover, BMHB samples exhibited good mechanical resistance, preventing damage during transportation, and remained stable at temperatures up to 150 °C. Furthermore, these materials were hydrophilic, with contact angles ranging from 35.6 \pm 0.6 to 64 \pm 5, and showed highly solubility in water regardless of pH conditions (up to 96.1 \pm 0.8). All these properties made BMHB samples highly suitable as packaging material for pesticides, such as acetamiprid, thus avoiding the need for direct handling of toxic substances. This innovative valorization approach not only provides a sustainable solution to manage sewage sludge into high-value products, but also contributes to the reduction of petroleum-derived plastics usage and the generation of wastes that often finds its way into water and soil.

Declaration of Competing Interest

The authors declare that they have no known competing financial interests or personal relationships that could have appeared to influence the work reported in this paper.

Data availability

Data will be made available on request.

Acknowledgements

The authors thank the financial support from the State Research Agency (Spanish Ministry of Science and Innovation) through the projects MCIU-19-RTI2018-094218-B-I00 and MCIU-22-PID2021-1259420B-I00, and for that received from the Foundation for the Promotion of Applied Scientific Research and Technology in Asturias through the project SV-PA-21-AYUD/2021/51041. Luis Romero acknowledges an FPI grant from the Spanish MICINN (PRE2019-091054).

Appendix A. Supplementary material

Supplementary data to this article can be found online at https://doi.org/10.1016/j.wasman.2023.11.022.

References

- Abelleira, Pérez-Elvira, S.I., Portela, J.R., Sánchez-Oneto, J., Nebot, E., 2012. Advanced thermal hydrolysis: Optimization of a novel thermochemical process to aid sewage sludge treatment. Environ. Sci. Technol. 46, 6158–6166.
- Adhikary, S.K., Ashish, D.K., Rudžionis, Ž., 2022. A review on sustainable use of agricultural straw and husk biomass ashes: Transitioning towards low carbon economy. Sci. Total Environ. 838, 156407.
- Agricultura, M. De, Alimentación, P., 1990. Real Decreto 1310. Spain.
- Alvarez, S., Weng, S., Alvarez, C., Marcet, I., Rendueles, M., Díaz, M., 2021. A new procedure to prepare transparent, colourless and low-water-soluble edible films using blood plasma from slaughterhouses 28.
- APHA, 2012. Standard Methods for examination of water and wastewater. American Public Health Association, Washington.
- Aragon-Briceño, C.I., Ross, A.B., Camargo-Valero, M.A., 2023. Strategies for the revalorization of sewage sludge in a waste water treatment plant through the integration of hydrothermal processing. Waste Biomass Valoriz. 14, 105–126.
- Ben, Z.Y., Samsudin, H., Yhaya, M.F., 2022. Glycerol: Its properties, polymer synthesis, and applications in starch based films. Eur. Polym. J. 175, 111377.

- Bien, J.B., Malina, G., Bien, J.D., Wolny, L., 2004. Enhancing anaerobic fermentation of sewage sludge for increasing biogas generation. J. Environ. Sci. Health A Tox. Hazard. Subst. Environ. Eng. 39, 939–949.
- Bracco, G., Holst, B., 2013. Surface science techniques, Springer Series in Surface Sciences
- Calva-Estrada, S.J., Jiménez-Fernández, M., Lugo-Cervantes, E., 2019. Protein-based films: advances in the development of biomaterials applicable to food packaging. Food Eng. Rev. 78–92.
- Celebi, H., Kurt, A., 2015. Effects of processing on the properties of chitosan/cellulose nanocrystal films. Carbohydr. Polym. 133, 284–293.
- Charles, A.L., Motsa, N., Abdillah, A.A., 2022. A Comprehensive Characterization of Biodegradable Edible Films Based on Potato Peel Starch Plasticized with Glycerol. Polymers (Basel) 14.
- Chen, L., Qiang, T., Chen, X., Ren, W., Zhang, H.J., 2022. Gelatin from leather waste to tough biodegradable packaging film: One valuable recycling solution for waste gelatin from leather industry. Waste Manag. 145, 10–19.
- European Commission, 2016. Final Renewal report for the active substance acetamiprid. Crichton, R.R., 2008. Structural and molecular biology for chemists. Biological Inorganic Chemistry. Elsevier 43–76.
- DuBois, M., Gilles, K.A., Hamilton, J.K., Rebers, P.A., Smith, F., 1956. Colorimetric method for determination of sugars and related substances. Anal. Chem. 28, 350–356.
- Elalami, D., Carrere, H., Monlau, F., Abdelouahdi, K., Oukarroum, A., Barakat, A., 2019. Pretreatment and co-digestion of wastewater sludge for biogas production: recent research advances and trends. Renew. Sustain. Energy Rev. 114, 109287.
- EurEau, 2021. Wastewater Treatment Sludge Management.
- Fang, Y.R., Li, S., Zhang, Y., Xie, G.H., 2019. Spatio-temporal distribution of sewage sludge, its methane production potential, and a greenhouse gas emissions analysis. J. Clean. Prod. 238, 117895.
- Fuertes, S., Laca, A., Oulego, P., Paredes, B., Rendueles, M., Díaz, M., 2017. Development and characterization of egg yolk and egg yolk fractions edible films. Food Hydrocoll. 70, 229–239.
- Gao, X., Dai, Y., Cao, J., Hou, H., 2023. Analysis of the effect mechanism of wet grinding on the film properties of pea protein isolate based on its structure changes. Innov. Food Sci. Emerg. Technol. 103474.
- Gao, J., Weng, W., Yan, Y., Wang, Y., Wang, Q., 2020. Comparison of protein extraction methods from excess activated sludge. Chemosphere 249, 126107.
- García, M., Urrea, J.L., Collado, S., Oulego, P., Díaz, M., 2017. Protein recovery from solubilized sludge by hydrothermal treatments. Waste Manag. 67, 278–287.
- García, M., Collado, S., Oulego, P., Díaz, M., 2020. The wet oxidation of aqueous humic acids. J. Hazard. Mater. 396, 122402.
- Giovanela, M., Parlanti, E., Soriano-Sierra, E.J., Soldi, M.S., Sierra, M.M.D., 2004. Elemental compositions, FT-IR spectral and thermal behavior of sedimentary fulvic and humic acids from aquatic and terrestrial environments. Geochem. J. 38, 255–264.
- González-Tolivia, E., Collado, S., Oulego, P., Díaz, M., 2022. BOF slag as a new alkalizing agent for the stabilization of sewage sludge. Waste Manag. 153, 335–346.
- Grube, M., Lin, J.G., Lee, P.H., Kokorevicha, S., 2006. Evaluation of sewage sludge-based compost by FT-IR spectroscopy. Geoderma 130, 324–333.
- Guan, R., Yuan, X., Wu, Z., Wang, H., Jiang, L., Li, Y., Zeng, G., 2017. Functionality of surfactants in waste-activated sludge treatment: a review. Sci. Total Environ. 609, 1433–1442.
- Guleria, A., Kumari, G., Lima, E.C., Ashish, D.K., Thakur, V., Singh, K., 2022. Removal of inorganic toxic contaminants from wastewater using sustainable biomass: a review. Sci. Total Environ. 823, 153689.
- Guo, L., Li, X.M., Bo, X., Yang, Q., Zeng, G.M., Liao, D. xiang, Liu, J.J., 2008. Impacts of sterilization, microwave and ultrasonication pretreatment on hydrogen producing using waste sludge. Bioresour. Technol. 99, 3651–3658.
- Gupta, S., Gajbhiye, V.T., Gupta, R.K., 2008. Effect of light on the degradation of two neonicotinoids viz acetamiprid and thiacloprid in soil. Bull. Environ. Contam. Toxicol. 81, 185–189.
- Guzman-Puyol, S., Benítez, J.J., Heredia-Guerrero, J.A., 2022. Transparency of polymeric food packaging materials. Food Res. Int. 161, 111792.
- Hui, W., Zhou, J., Jin, R., 2022. Proteins recovery from waste activated sludge by thermal alkaline treatment. J. Environ. Chem. Eng. 10, 107311.
- Ishak, Z.I., Sairi, N.A., Alias, Y., Aroua, M.K.T., Yusoff, R., 2016. Production of glycerol carbonate from glycerol with aid of ionic liquid as catalyst. Chem. Eng. J. 297, 128–138.
- Jakob, L., Mokdad, H., Wyser, Y., 2002. Understanding puncture resistant and perforation behavior of packaging laminates. J. Plast. Film Sheeting.
- Junaidi, Y., Windari, W., Aini, F.N., 2022. Nutrient content of super liquid fertilizer (SLF) from dairy sludge waste and the potential as a biopesticide i.
- Kacprzak, M., Neczaj, E., Fijałkowski, K., Grobelak, A., Grosser, A., Worwag, M., Rorat, A., Brattebo, H., Almås, Å., Singh, B.R., 2017. Sewage sludge disposal strategies for sustainable development. Environ. Res. 156, 39–46.
- Kang, X.R., Zhang, G.M., Chen, L., Dong, W.Y., Tian, W.D., 2011. Effect of initial pH adjustment on hydrolysis and acidification of sludge by ultrasonic pretreatment. Ind. Eng. Chem. Res. 50, 12372–12378.
- Lowry, OliverH, Rosebrough, NiraJ, Farr, A.L., Randall, RoseJ, 1951. Protein measurement with the folin phenol reagent. J. Biol. Chem. 193, 265–275
- Marcet, I., Sáez, S., Rendueles, M., Díaz, M., 2017. Edible films from residual delipidated egg yolk proteins. J. Food Sci. Technol. 54, 3969–3978.
- Mellor, J.D., Bell, G.A., 1993. FREEZE-DRYING The Basic Process.
- Nagarajan, M., Benjakul, S., Prodpran, T., Songtipya, P., Kishimura, H., 2012. Characteristics and functional properties of gelatin from splendid squid (Loligo

- formosana) skin as affected by extraction temperatures. Food Hydrocoll. 29, 389-397.
- Nordin, N., Othman, S.H., Rashid, S.A., Basha, R.K., 2020. Effects of glycerol and thymol on physical, mechanical, and thermal properties of corn starch films. Food Hydrocoll. 106, 105884.
- Pelton, J.T., McLean, L.R., 2000. Spectroscopic methods for analysis of protein secondary structure. Anal. Biochem. 277, 167–176.
- Phogat, A., Singh, J., Kumar, V., Malik, V., 2022. Toxicity of the acetamiprid insecticide for mammals: a review. Environ. Chem. Lett. 20, 1453–1478.
- Pirsa, S., Farshchi, E., Roufegarinejad, L., 2020. Antioxidant/antimicrobial film based on carboxymethyl cellulose/gelatin/TiO2–Ag nano-composite. J. Polym. Environ. 28, 3154–3163
- Pola, L., Fernández-García, L., Collado, S., Oulego, P., Díaz, M., 2021. Heavy metal solubilisation during the hydrothermal treatment of sludge. J. Environ. Manage. 206
- Pola, L., Collado, S., Oulego, P., Díaz, M., 2022. A proposal for the classification of sludge products throughout hydrothermal treatment. Chem. Eng. J. 430, 132746.
- Romero, L., Oulego, P., Collado, S., Díaz, M., 2023. Advanced thermal hydrolysis for biopolymer production from waste activated sludge: Kinetics and fingerprints. J. Environ. Manage. 342, 118243.
- Ruiz-Hernando, M., Cabanillas, E., Labanda, J., Llorens, J., 2015. Ultrasound, thermal and alkali treatments affect extracellular polymeric substances (EPSs) and improve waste activated sludge dewatering. Process Biochem. 50, 438–446.
- Sankaran, S., Ehsani, R., 2014. Introduction to the electromagnetic spectrum. In: Imaging with Electromagnetic Spectrum. Springer, Berlin Heidelberg, pp. 1–15.
- Seviour, T., Derlon, N., Dueholm, M.S., Flemming, H.-C., Girbal-Neuhauser, E., Horn, H., Kjelleberg, S., van Loosdrecht, M.C.M., Lotti, T., Malpei, M.F., Nerenberg, R., Neu, T. R., Paul, E., Yu, H., Lin, Y., 2019. Extracellular polymeric substances of biofilms: Suffering from an identity crisis. Water Res. 151, 1–7.
- Shanmathy, M., Mohanta, M., Thirugnanam, A., 2021. Development of biodegradable bioplastic films from Taro starch reinforced with bentonite. Carbohydrate Polymer Technologies and Applications 2.
- Simon, S., Païro, B., Villain, M., D'Abzac, P., Hullebusch, E.V., Lens, P., Guibaud, G., 2009. Evaluation of size exclusion chromatography (SEC) for the characterization of extracellular polymeric substances (EPS) in anaerobic granular sludges. Bioresour. Technol. 100, 6258–6268.
- Socrates, G., 2003. Infrared and Raman Characteristic Group Frequencies: Tables and Charts. John Wiley & Sons Ltd.
- Song, N.-B., Jo, W.-S., Song, H.-Y., Chung, K.-S., Won, M., Song, K.B., 2013. Effects of plasticizers and nano-clay content on the physical properties of composite films. Food Hydrocoll. 31, 340–345.

- Song, X., Shi, Z., Li, X., Wang, X., Ren, Y., 2019. Fate of proteins of waste activated sludge during thermal alkali pretreatment in terms of sludge protein recovery. Front. Environ. Sci. Eng. 13, 25.
- Thomas, A.P., Kasa, V.P., Dubey, B.K., Sen, R., Sarmah, A.K., 2023. Synthesis and commercialization of bioplastics: organic waste as a sustainable feedstock. Sci. Total Environ. 904, 167243.
- Urrea, J.L., Collado, S., Laca, A., Díaz, M., 2015. Rheological behaviour of activated sludge treated by thermal hydrolysis. J. Water Process Eng. 5, 153–159.
- Urrea, J.L., Collado, S., Oulego, P., Díaz, M., 2016. Effect of wet oxidation on the fingerprints of polymeric substances from an activated sludge. Water Res. 105, 282–290.
- Urrea, J.L., Collado, S., Oulego, P., Díaz, M., 2017a. Formation and degradation of soluble biopolymers during wet oxidation of sludge. ACS Sustain. Chem. Eng. 5, 3011–3018.
- Urrea, J.L., Collado, S., Oulego, P., Díaz, M., 2017b. Wet oxidation of the structural sludge fractions. J. Clean. Prod. 168, 1163–1170.
- Urrea, J.L., García, M., Collado, S., Oulego, P., Díaz, M., 2018. Sludge hydrothermal treatments. Oxidising atmosphere effects on biopolymers and physical properties. J. Environ. Manage. 206, 284–290.
- van Veenhuyzen, B., Tichapondwa, S., Hörstmann, C., Chirwa, E., Brink, H.G., 2021. High capacity Pb(II) adsorption characteristics onto raw- and chemically activated waste activated sludge. J. Hazard. Mater. 416, 125943.
- Wang, H., Cai, W.W., Liu, W.Z., Li, J.Q., Wang, B., Yang, S.C., Wang, A.J., 2018. Application of sulfate radicals from ultrasonic activation: disintegration of extracellular polymeric substances for enhanced anaerobic fermentation of sulfatecontaining waste-activated sludge. Chem. Eng. J. 352, 380–388.
- World Economic Forum, 2016. The New Plastics Economy Rethinking the Future of Plastics. Switzerland, Geneva, p. 16.
- Xue, Y., Liu, H., Chen, S., Dichtl, N., Dai, X., Li, N., 2015. Effects of thermal hydrolysis on organic matter solubilization and anaerobic digestion of high solid sludge. Chem. Eng. J. 264, 174–180.
- Yang, H.-J., Lee, J.-H., Won, M., Song, K.B., 2016. Antioxidant activities of distiller dried grains with solubles as protein films containing tea extracts and their application in the packaging of pork meat. Food Chem. 196, 174–179.
- Zhang, C., Wang, C., Cao, G., Wang, D., Ho, S.-H., 2020. A sustainable solution to plastics pollution: an eco-friendly bioplastic film production from high-salt contained Spirulina sp. residues. J. Hazard. Mater. 388, 121773.
- Zhong, Y., Zhuang, C., Gu, W., Zhao, Y., 2019. Effect of molecular weight on the properties of chitosan films prepared using electrostatic spraying technique. Carbohydr. Polym. 212, 197–205.